Electronic Supplementary Material (ESI) for Chemical Science.

Tuning reactivity layer-by-layer: Formic Acid Activation on Ag/ Pd(111)

Supplementary Information

Mustafa Karatok[a], Kaining Duanmu[b], Christopher R. O'Connor[a], Jorge Anibal Boscoboinik[c], Philippe Sautet[b], Robert J. Madix[d], Cynthia M. Friend*[a,d]

[a]Department of Chemistry and Chemical Biology, Harvard University, Cambridge, MA 02138, USA

[b]Department of Chemical and Biomolecular Engineering, University of California, Los Angeles, California 90095, United States

[d]Center for Functional Nanomaterials, Brookhaven National Laboratory, Upton, NY, 11973, USA

[d]John A. Paulson School of Engineering and Applied Sciences, Harvard University, Cambridge, MA 02138, USA

Quantification of the Ag coverage on Pd(111) based on XPS and AES

An n-layer overlayer model was used to calculate θ, the Ag coverage with normal photoelectron emission. The value of n in the n-layer model is chosen where, $n < \theta < n + 1$.

$$\frac{I_{Ag,corrected}}{I_{Pd,corrected}} = \frac{1 - \big(\theta - (n)\big)\exp\left[\frac{-(n+1)d}{\lambda_{Ag,KE=Ag}}\right] - \big((n+1) - \theta\big)\exp\left[\frac{-(n)d}{\lambda_{Ag,KE=Ag}}\right]}{\big(\theta - (n)\big)\exp\left[\frac{-(n+1)d}{\lambda_{Ag,KE=Pd}}\right] + \big((n+1) - \theta\big)\exp\left[\frac{-(n+1)d}{\lambda_{Ag,KE=Pd}}\right]}$$

XPS using monochromatic Al Kα (hv = 1468.7 eV)

The measured $Pd3d_{5/2}$ and $Ag3d_{5/2}$ peak areas were corrected with

$$I_{Pd,corrected} = \frac{I_{Pd,measured}}{\sigma_{Pd} \cdot \lambda_{Pd,KE=1151.7eV} \cdot \rho_{Pd} \cdot T_{KE=1151.7eV}}$$

$$I_{Ag,corrected} = \frac{I_{Ag,measured}}{\sigma_{Ag} \cdot \lambda_{Ag,KE=1118.5eV} \cdot \rho_{Ag} \cdot T_{KE=1118.5eV}}$$

The ionization cross sections were corrected for the angular dependence, by multiplying with

$$1 - \frac{\beta}{2} P_2(cos\alpha)$$

In this formula, α is the angle between the incident unpolarized photon beam and the emitted photoelectrons, which was close to 43° and $P_2(x) = 0.5(3x^2 - 1)$. [1,2]

Table S1. Element and kinetic-energy dependent parameters used for estimating the Pd coverage based on the measured Ag/Pd ratio determined from UHV XPS. Photon flux was constant.

	Pd (KE = 1151.7 eV)	**Ag (KE = 1118.5 eV)**
σ, ionization cross section / Mbarn [3]	0.220	0.248
β, asymmetry parameter [3]	1.21	1.21
λ_{Pd}, inelastic mean free path in Pd / nm [4]	1.50	1.46
λ_{Ag}, inelastic mean free path in Ag / nm [4]	1.59	1.55
ρ, atomic density / atoms nm^{-3}	67.9	58.6
T, transmission factor	1.00	1.00
a, lattice parameter /nm	0.389	0.409
332d, layer (111) thickness (d√3/3) / nm	0.225	0.236

AES using 2 kV electron beam

The measured amplitudes of differentiated signal of the Pd MNN Auger and Ag MNN Auger were corrected with

$$I_{Pd,corrected} = \frac{I_{Pd,measured}}{S_{Pd}}$$

$$I_{Ag,corrected} = \frac{I_{Ag,measured}}{S_{Ag}}$$

Table S2. Element and kinetic-energy dependent parameters used for estimating the Pd coverage based on the measured Ag/Pd ratio determined from UHV XPS. Photon flux was constant.

	Pd (KE = 324.0 eV)	**Ag (KE = 349.0 eV)**
S, AES sensitivity factor [5]	0.220	0.248
λ_{Ag}, inelastic mean free path in Ag / nm [4]	0.68	0.71
a, lattice parameter /nm	0.389	0.409
332d, layer (111) thickness (d$\sqrt{}$3/3) / nm	0.225	0.236

Slab models used in DFT calculations

The structure of Ag(111) and Ag/Pd(111) slab models used in the DFT calculations are given in Figure S1. Table S3 and S4 show the calculated Ag3d core level shifts (CLS), Ag chemical potentials (μ_{Ag}) and d-band center in various slab models by using both the Ag and Pd lattice constants for the Ag overlayer. The chemical potential of surface Ag in Ag/Pd(111) is calculated as μ_{Ag} =[E(Ag/Pd(111))–E(5-layer Pd(111))]/n_{Ag}, where n_{Ag} is the number of surface Ag atoms.

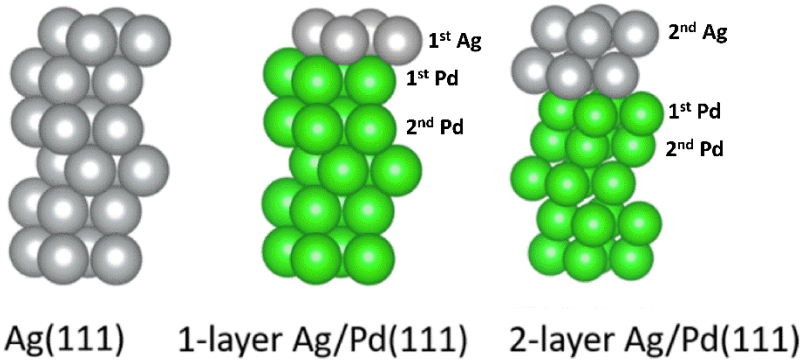

Figure S1. The structure of Ag(111) and Ag/Pd(111) slab models used in the DFT calculations (Grey: Ag, Green: Pd).

Table S3. The surface Ag3d core level shifts (CLS) and Ag chemical potentials calculated with DFT for various slab models.

Slab model	Surface Ag3d CLS (eV)	Ag chemical potential (eV)
Ag(111)	-0.08	-
1-layer Ag/Pd(111) in Ag lattice	-0.23	-3.05
2-layer Ag/Pd(111) in Ag lattice	-0.05	-2.91
1-layer Ag/Pd(111) in Pd lattice	-0.15	-2.97
2-layer Ag/Pd(111) in Pd lattice	-0.01	-2.84

Table S4. The d-band centers (eV) of Ag and Pd layers in various slab models.

Slab model	Ag(111)		Pd(111)	1-layer Ag/Pd(111)		2-layer Ag/Pd(111)	
	Ag lattice	Pd lattice	Pd lattice	Ag lattice	Pd lattice	Ag lattice	Pd lattice
Surface Ag	-3.85	-3.94					
Surface Pd			-4.19				
1st Ag layer				-3.65	-3.83		
2nd Ag layer						-4.02	-4.08
1st Pd layer				-1.40	-1.55	-1.68	-1.76
2nd Pd layer				-1.66	-1.69	-1.81	-1.90

Calculated density of states (DOS) of Ag/Pd(111)

The calculated density of states (DOS) of the d-orbitals of the Ag and Pd layers in the 1-layer Ag/Pd(111) slab model is determined by using both the Ag (Figure S2-a) and Pd (Figure S2-b) lattice constants.

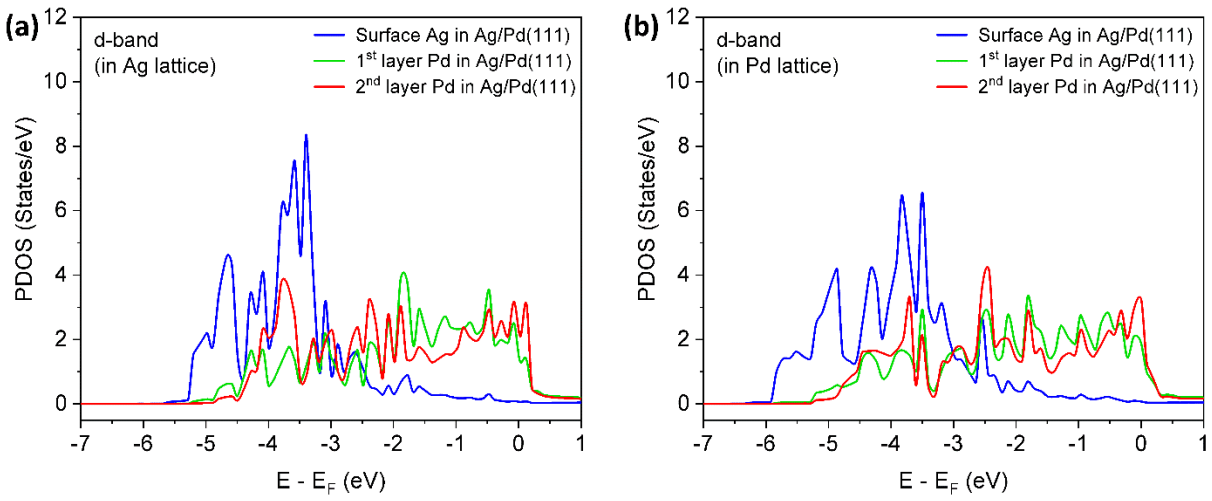

Fig S2. The density of states (DOS) of the d-orbitals of Ag and Pd layers in the 1-layer Ag/Pd(111) slab model. (a) Ag and (b) Pd lattice constants were used in the calculations.

Infrared Reflection Absorption Spectra

The effect of adsorption of background CO on Pd(111) at 300 K contributes to the imperfect background subtraction in the data. Two consecutive infrared spectra of Pd(111) were taken at 300 K and subtracted from each other (Figure S3-a). The adsorption of background CO in a three-fold hollow geometry during the time period of data acquisition for the second spectrum was obtained at 1846 cm^{-1} (Figure S3-a). Subsequently, after a 1.5 L exposure of CO there is a more intense CO signal at 1924 cm^{-1} indicating more CO adsorption in a bridging geometry on Pd(111) (Figure S3-b). A transition from threefold-hollow to bridge sites with increasing CO coverage has been previously reported [6]. Thus, the positive signal at ~1846 cm^{-1} in spectrum-b is attributed to background CO adsorption (three-fold hollow) that was subtracted from the data.

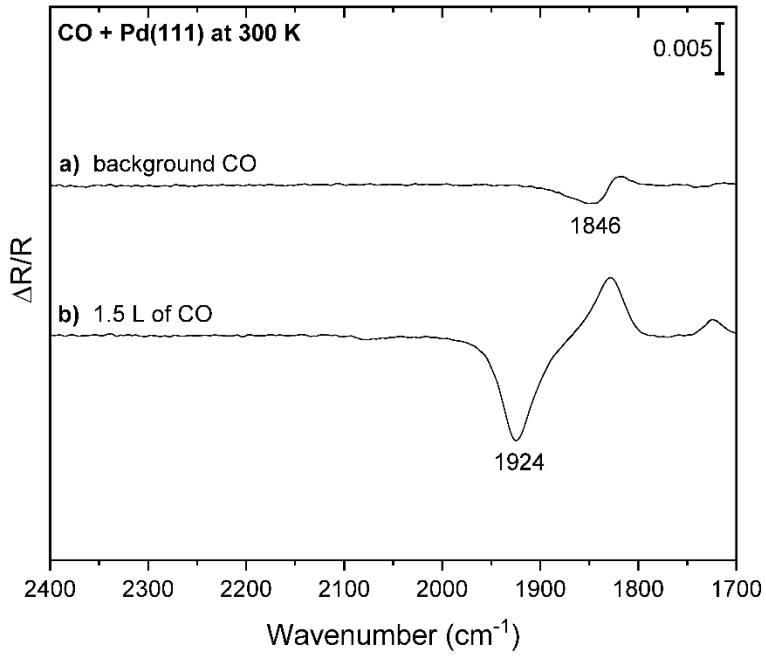

Figure S3. Infrared Reflection Absorption Spectra (IRRAS) shows the effect of background CO adsorption on the imperfect background subtraction. IRRAS spectra obtained on clean Pd(111) at 300 K a) after background CO adsorption between two consecutive spectrum acquisition and b) following a 1.5 L of CO exposure.

Curve fitting procedure for the spectrum given in Figure 2c

The background was corrected with a Shirley-type [7] background prior to the curve fitting procedure of the X-ray photoelectron spectrum of Ag(2.9 ML)/Pd(111) provided in Figure 2c and Figure S4. The line shape and width of the spectrum in Figure 2d was determined by using clean Ag(111) as a reference for the fitting parameters. Two peaks centered at 368.0 (shaded green) and 368.3 eV (shaded grey) shows the first layer of Ag at the Pd-Ag interface and multilayers of Ag without Pd neighbors, respectively. The integrated area of the first Ag layer signal (shaded green) was found 37% of the total Ag signal.

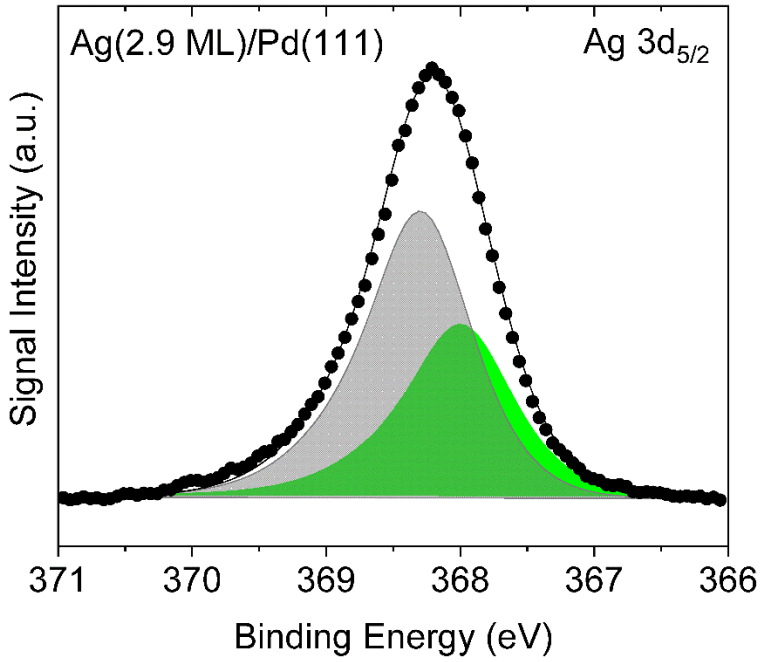

Figure S4. Ag $3d_{5/2}$ X-ray photoelectron spectrum obtained after deposition of 2.9 ML of Ag on Pd(111) at 300 K (black points). The spectrum was deconvoluted to two peaks centered at 368.0 and 368.3 eV which are attributed to first Ag layer at the Pd-Ag interface (shaded green) and Ag in multilayers (shaded grey), respectively. Sum of the two fits is given by a black solid line.

Photoelectron spectroscopy Ag layer analysis

An n-layer overlayer model was used to calculate the ratio of interfacial Ag (1st layer Ag) to total Ag to determine the self-consistency of the structural model used and the Ag3d peak fit intensities for 2.9 ML Ag/Pd(111).

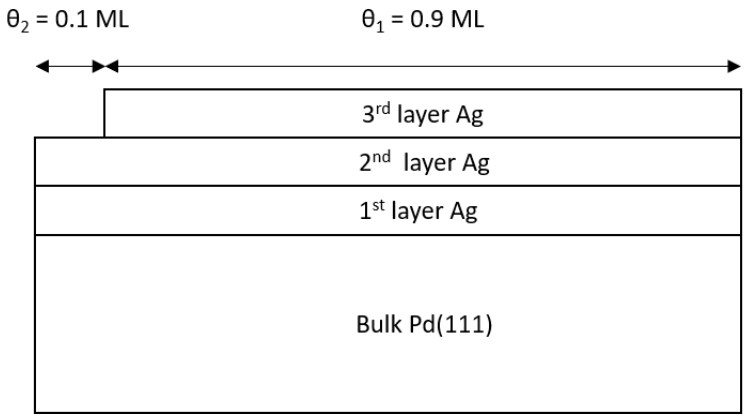

Figure S5. Model for layer-by-layer growth of 2.9 ML Ag deposited on Ag(111).

The predicted intensity of the Ag3d signal for a surface layer of Ag is given by:

$$\frac{I_{Ag3d}^{n=0}}{I_o} = 1 - \exp\left[\frac{d}{\lambda_{Ag,KE=Ag}}\right] = 0.141$$

The predicted intensity of the Ag3d signal for a layer of Ag attenuated by one layer of Ag is given by:

$$\frac{I_{Ag3d}^{n=1}}{I_o} = 1 - \exp\left[\frac{2d}{\lambda_{Ag,KE=Ag}}\right] - \frac{I_{Ag3d}^{n=0}}{I_o} = 0.122$$

The predicted intensity of the Ag3d signal for a layer of Ag attenuated by two layers of Ag is given by:

$$\frac{I_{Ag3d}^{n=2}}{I_o} = 1 - \exp\left[\frac{3d}{\lambda_{Ag,KE=Ag}}\right] - \frac{I_{Ag3d}^{n=0}}{I_o} - \frac{I_{Ag3d}^{n=1}}{I_o} = 0.104$$

Table S5. Element and kinetic-energy dependent parameters used for estimating the Ag layer ratio to total Ag based on the measured Ag3d determined from XPS. Photon flux was constant.

	Ag (KE = 1118.5 eV)
λ_{Ag}, inelastic mean free path in Ag / nm [4]	1.55
a, lattice parameter /nm	0.409
332d, layer (111) thickness (d√3/3) / nm	0.236

Using the model depicted in Figure S1, the intensity of each layer of Ag is calculated.

The predicted intensity of 1st layer Ag is given by:

$$\frac{I_{1st\ Ag}}{I_o} = \theta_1 \cdot \frac{I_{Ag3d}^{n=2}}{I_o} + \theta_2 \cdot \frac{I_{Ag3d}^{n=1}}{I_o} = 0.106$$

The predicted intensity of 2nd layer Ag is given by:

$$\frac{I_{2nd\ Ag}}{I_o} = \theta_1 \cdot \frac{I_{Ag3d}^{n=1}}{I_o} + \theta_2 \cdot \frac{I_{Ag3d}^{n=0}}{I_o} = 0.124$$

The predicted intensity of 3rd layer Ag is given by:

$$\frac{I_{3rd\ Ag}}{I_o} = \theta_1 \cdot \frac{I_{Ag3d}^{n=0}}{I_o} = 0.127$$

The model predicts that for 2.9 ML of Ag deposited on Pd(111), the Ag3d area ratio of interfacial Ag (1st layer Ag) to total Ag is 0.30 which is in reasonable agreement with the experimental value (0.37).

Valence band structure by X-ray photoelectron spectroscopy

A change in the valence band structure of Ag/Pd(111) relative to bulk Ag(111) was determined by X-ray photoelectron spectroscopy (Figure S6). Figure S6a (θ_{Ag} = 1.1 ML) and S6c (θ_{Ag}= 2.9 ML) show the valence band spectra of Ag/Pd(111) (black dots), along with that of pristine Pd(111) (shaded green), Ag(111) (shaded gray) and a linear combination of the clean surfaces (red). To visualize the change in valence band structure for a Ag overlayer, the Pd(111) contribution was subtracted from the data obtained for Ag/Pd(111) (Figure S6b and S6d). The result shows an increase in the density of states in the range of -0.3 eV-E_F for a monolayer Ag on Pd compared to Ag(111), and a lack of change in the same region for multilayer Ag on Pd(111) which is in agreement with the calculations presented in the main text (Figure 3a).

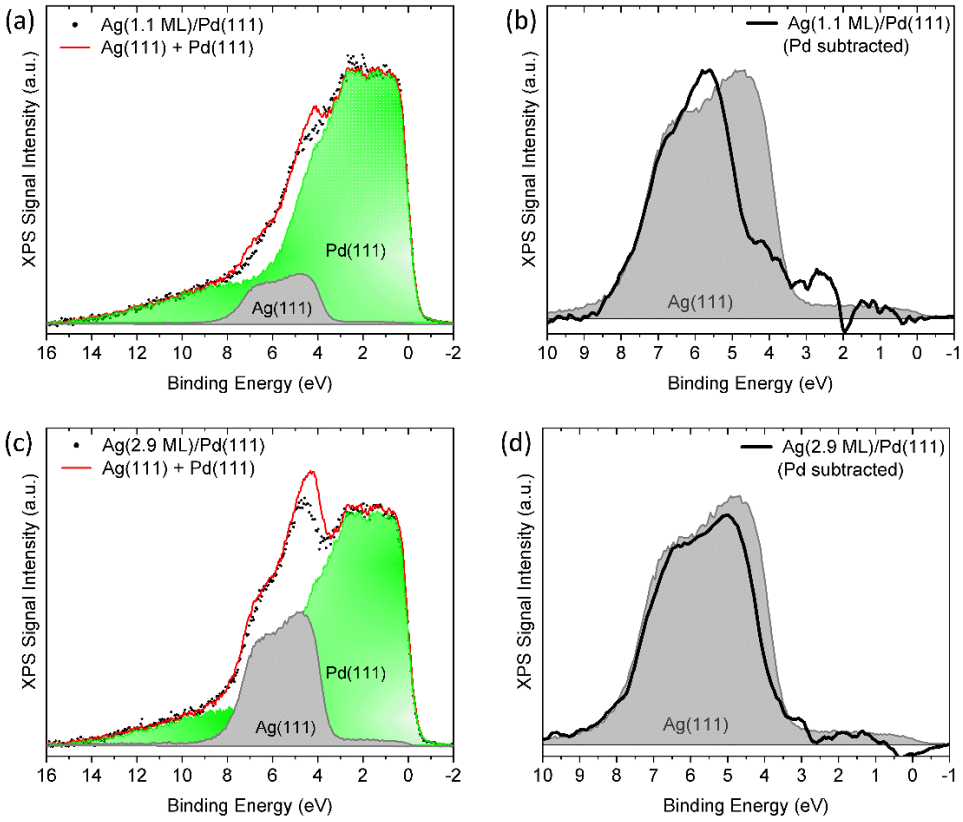

Figure S6. The change in the valence band structure of Ag monolayers was shown by X-ray photoelectron spectroscopy (XPS). Photoelectron spectra were obtained for Ag(111) (shaded grey), Pd(111) (shaded green), Ag(1.1 ML)/Pd(111) (black dot in panel a) and Ag(2.9 ML)/Pd(111) (black dot in panel c). A linear combination of Ag(111) and Pd(111) was given in panel a and c (red). A pristine Pd(111) contribution to Ag/Pd(111) spectra was subtracted and given in panel b and d (black) along with clean Ag(111) (shaded grey).

Temperature Programmed Reaction Data

The decomposition of formic acid (HCOOH) on clean Pd(111) yields CO_2 and H_2O at 190 K, H_2 at 310 K, and CO at 460 K (Figure S7) as evidenced by temperature programmed reaction. A small m/z=46 signal (a fragment of formic acid in quadrupole mass spectrometer) obtained at 190 K was attributed to either unreacted formic acid or a recombinative desorption of the products. Multilayers of formic acid sublime at ~160 K (m/z=46 and 44).

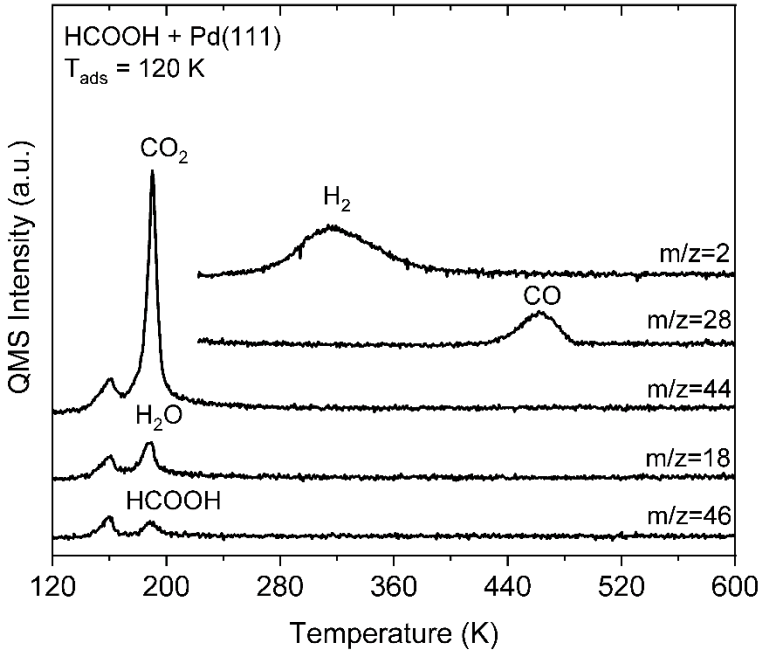

Figure S7. Temperature programmed reaction data for HCOOH on clean Pd(111). Data were obtained after exposure of formic acid (0.03 L) to Pd(111) at 120 K followed by linear heating. The heating rate was 1 K/s. The data are not corrected for fragmentation in the mass spectrometer. The formic acid fragmentation of m/z=44:46 was determined as ~1:1.2.

In order to eliminate the interference of background H_2 adsorption on the m/z=2 signal, d_2-formic acid (DCOOD) adsorption was carried out on clean and Ag containing Pd(111) at 120 K, and m/z=3 and m/z=4 signals were monitored by temperature programmed reaction experiments (Figure S8). Mainly m/z=3 signals were obtained along with a negligible m/z=4 signal due to dissociative H_2 adsorption from the background. In addition to the HD desorption at 315 K on clean Pd(111), an additional shoulder at ~250 K was obtained for Ag(0.8 ML)/Pd(111) indicating HD desorption from Ag containing domains.

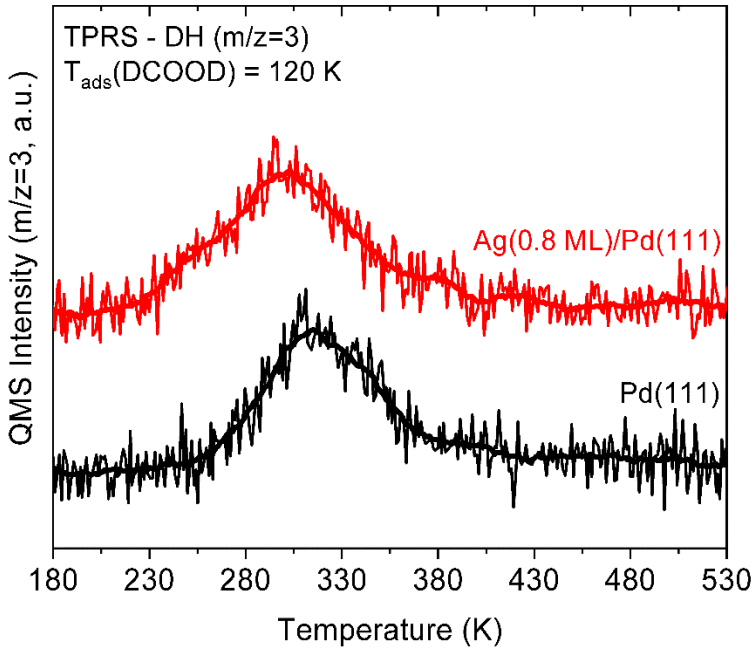

Figure S8. Production of HD (m/z=3) during temperature programmed reaction of DCOOD on Ag(0.8 ML)/Pd(111) (red) and clean Pd(111) (black) peaks. The HD peaks at ~280 K for reaction on Ag(0.8 ML)/Pd(111) (red), is nearly coincident with CO_2 formation. HD is evolved from DCOOD reaction on a clean Pd(111) (black) in a peak at ~330 K, which is desorption-limited. The formation of HD instead of D_2 or H_2, shows that there is a source of adsorbed H in both cases. Possible sources of adsorbed H is from background H_2 dissociation or from exchange of the deuterium in DCOOD with the chamber walls during dosing. Ag was deposited on Pd(111) at 300 K prior to DCOOD exposure (0.03 L) to the surfaces at 120 K. The heating rate is 1 K/s. The data was not corrected for fragmentation in the mass spectrometer.

In order to differentiate background CO adsorption from CO produced by formic acid decomposition, ^{13}C-formic acid (H^{13}COOH) adsorption was carried out on clean and Ag containing Pd(111) at 120 K, and m/z=29 signal was monitored in temperature programmed reaction experiments (Figure S9). Temperature programmed reaction spectra in Figure S9 shows that the ^{13}CO signal observed at 485 K for Pd(111) was diminished and slightly shifted to lower temperature for Ag(1.0 ML)/Pd(111). These results indicate that the total carbon monoxide production by formic acid decomposition is decreased for a Ag monolayer on Pd(111).

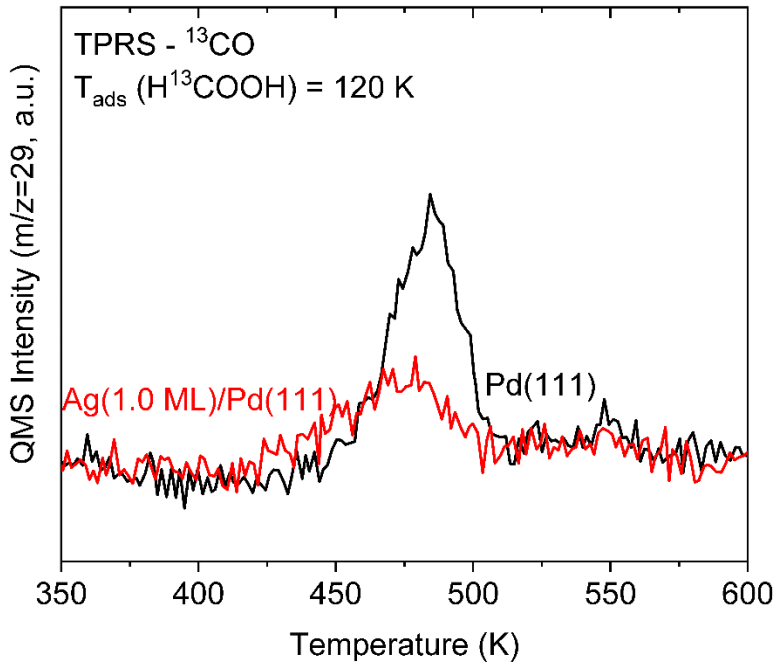

Figure S9. Temperature programmed reaction profiles of ^{13}CO produced from the decomposition of H^{13}COOH on clean Pd(111) (black) and on Ag(1.0 ML)/Pd(111) (red). The Ag layer was deposited at 300 K. The H^{13}COOH (0.03 L) was exposed to both surfaces at 120 K. The heating rate was 1K/s. The data was not corrected for fragmentation in the mass spectrometer.

References

[1] Kennedy, D.J. and Manson, S.T., 1972. Photoionization of the noble gases: cross sections and angular distributions. *Physical Review A*, *5*(1), p.227.

[2] Cooper, J.W. and Manson, S.T., 1969. Photo-ionization in the soft X-ray range: angular distributions of photoelectrons and interpretation in terms of subshell structure. *Physical Review*, *177*(1), p.157.

[3] Data adapted from https://vuo.elettra.eu/services/elements/WebElements.html

[4] Shinotsuka, H., Tanuma, S., Powell, C.J. and Penn, D.R., 2015. Calculations of electron inelastic mean free paths. X. Data for 41 elemental solids over the 50 eV to 200 keV range with the relativistic full Penn algorithm. *Surface and Interface Analysis*, *47*(9), pp.871-888.

[5] Davis, L.E., MacDonald, N.C., Palmberg, P.W., Riach, G.E. and Weber, R.E., 1976. Handbook of Auger Electron Spectroscopy, Physical Electronics Industries. *Inc., Eden Prairie, Minnesota*, pp.1-12.

[6] Ma, Y., Diemant, T., Bansmann, J. and Behm, R.J., 2011. The interaction of CO with PdAg/Pd (111) surface alloys—A case study of ensemble effects on a bimetallic surface. *Physical Chemistry Chemical Physics*, *13*(22), pp.10741-10754.

[7] Shirley, D.A., 1972. High-resolution X-ray photoemission spectrum of the valence bands of gold. *Physical Review B*, *5*(12), p.4709.